

Effect of the surface expansion and wettability of the capillary on the dynamic surface tension measured by the maximum bubble pressure method

T.S. Horozov ^{a,*}, C.D. Dushkin ^a, K.D. Danov ^a, L.N. Arnaudov ^a, O.D. Velev ^a,
A. Mehreteab ^b, G. Broze ^c

^a *Laboratory of Thermodynamics and Physicochemical Hydrodynamics, Faculty of Chemistry, University of Sofia, 1126 Sofia, Bulgaria*

^b *Colgate–Palmolive Technology Center, 909 River Road, Piscataway, NJ 08854-5596, USA*

^c *Colgate–Palmolive Research and Development, Inc., Avenue Du Parc Industriel, B-4041 Milmort (Herstal), Belgium*

Received 5 October 1995; accepted 15 February 1996

Abstract

The dynamic surface tension (DST) of sodium dodecyl sulfate solutions in the presence of sodium chloride is studied by the maximum bubble pressure method. The pressure oscillations are measured with a pressure transducer, while the change of the bubble area with time is determined by means of a video system. The role of the wettability of the capillary is studied by means of measurements with hydrophilic and hydrophobic capillaries. A strong effect of wettability of the capillary on the bubble growth and the DST is observed. The DST data are interpreted with a model for diffusion-controlled adsorption assuming different laws of bubble expansion. The real law of expansion is found to be important for correct interpretation in the case of the hydrophobic capillary. However, the surface expansion is not of primary importance for interpretation of the DST data obtained with the hydrophilic capillary. It is proved that the maximum pressure does not correspond to the hemispherical shape of the bubble in the presence of surfactant. Neglecting this effect does not lead to a significant error in the DST for bubbling periods smaller than several seconds.

Keywords: Bubble growth; Dynamic surface tension; Hydrophilic capillary; Hydrophobic capillary; Maximum bubble pressure method; Surface expansion; Wettability

1. Introduction

The maximum bubble pressure method (MBPM) is one of the classical experimental techniques for the measurement of the dynamic surface tension (DST) of surfactant solutions [1]. The

DST is calculated from the maximum pressure applied in blowing consecutive air bubbles at the tip of a capillary immersed in the solution. This method is widely used in practice due to its experimental simplicity and the possibility for DST measurements over a wide time range from approximately 10 ms up to hours. Recently, some commercial automated set-ups have even been built [2].

* Corresponding author.

Nevertheless, some aspects of the method still remain not very clear.

1.1. Expansion of the bubble surface

There have been several experimental studies of bubble growth performed by high-speed cinematography [1,3,4]. Bendure [3] has studied the DST of non-ionic surfactant solutions by MBPM with a hydrophilic glass capillary. He pointed out that the solution entered the capillary after the detachment of each bubble. Based on photographs, he claimed that the dynamic surface tension data corresponded to an essentially constant interfacial area. He interpreted the DST data by diffusion theory [5], which does not account for surface expansion. The diffusion coefficients obtained by him, however, have been 5–10 times lower than the expected value of $5 \times 10^{-6} \text{ cm}^2 \text{ s}^{-1}$. The presence of convective mass transfer has been indicated by him as a possible reason for such a disagreement. Garret and Ward [4] have studied the growth of bubbles at the tip of a hydrophilic glass capillary in a similar way to Bendure. Their attention has been focused mainly on the fast spontaneous expansion of the bubbles before detachment from the capillary. The early stages of the expansion preceding the moment of a hemispherical bubble have not been studied in detail. The authors just pointed out that the bubble area has not been significantly changed during this stage. They interpreted the DST data assuming a constant area of the bubble, and found satisfactory agreement between measured DSTs and diffusion theory [5] for solutions of sodium dodecyl sulfate (SDS) and some other anionic and zwitterionic surfactants. Joos and Rillaerts [6] have reinterpreted Bendure's data assuming that bubbles expand under a constant flow rate. They have obtained much better diffusivities than Bendure and stressed that the surface expansion should be taken into account for the interpretation of DST data. Other workers have obtained reasonable results assuming a linear expansion of the bubble surface [7,8]. However, their assumptions have not been based on experiment. Consequently, the real law of bubble surface expansion and its importance for the interpretation of DST data still remain not very clear.

1.2. The wettability of the capillary

Hydrophilic glass capillaries are usually used in maximum bubble pressure experiments. It is well known that the solution enters such capillaries just after the detachment of each bubble [3,4]. Mysels [1] was probably the first to point out that this phenomenon complicates the theoretical interpretation of the experimental data. To avoid this problem, he used a hydrophobic capillary with a hydrophilic tip. However, whether the DST depends on the wettability of the capillary is still an open question.

1.3. Does the maximum pressure correspond to a hemispherical shape of the bubble?

A positive answer to this question seems obvious in the case of pure liquids. However, this is not so in the presence of surfactant since both the bubble radius and the surface tension change during the expansion of the bubble. Garret and Ward [4] have shown by theoretical considerations that the maximum pressure may not correspond to a hemispherical shape of the bubble in surfactant solutions. They have noted that if such an effect exists, it should be more pronounced at low bubbling frequencies (i.e. for long bubbling periods). However, they have not proved this conclusion by experiment with any degree of certainty.

The present work aims to elucidate the unclear aspects of the MBPM cited above.

2. Experiment

2.1. Experimental set-up

In order to measure the dynamic surface tension, we have constructed the experimental set-up shown in Fig. 1. The peristaltic pump compresses air into a reservoir of volume approximately 500 cm^3 . The pressure inside the reservoir is kept at approximately $7 \times 10^5 \text{ dyn cm}^{-2}$. Valve 1 serves to control the outflow of air from the reservoir, thus the adjustment of the bubbling frequency. The compressed air enters a chamber whose volume can be varied gradually by means of a syringe, from about

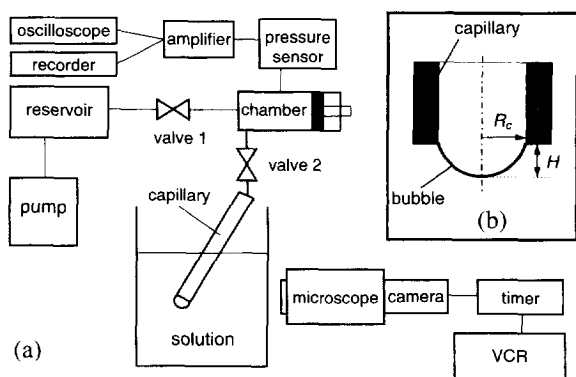


Fig. 1. (a) Scheme of the experimental set-up; (b) cross-section of the capillary.

0.5 to 50 cm³. By changing the chamber volume, one can enhance (low chamber volume) or damp (high chamber volume) the oscillations of the pressure inside the system. The variation of pressure is detected by means of a piezoresistive pressure transducer (Micro Switch). The output electrical signal is amplified and then registered by a digital storage oscilloscope (Tektronix) and chart recorder (Radelkis, Hungary; designed for polarography). The chart recorder can work in the peak mode, which allows the measurement of the maximum output voltage even at high bubbling frequencies. The capillary is immersed in the liquid at an angle of about 30° with respect to the liquid surface. Use of an inclined capillary leads to a more stable bubbling frequency than a vertical capillary [9]. The capillary is connected to the chamber by flexible plastic tubing. To control the resistance of the capillary, another valve (valve 2) is mounted as close as possible to the capillary end. The process of bubbling is observed by a long-focus microscope equipped with a CCD camera. The video image is recorded by a Super VHS recorder (Sony). The real time of the experiment is also stored simultaneously by using an electronic timer. The temperature of the solution is controlled by a thermostat and was maintained at $30.6 \pm 0.1^\circ\text{C}$ in all experiments.

2.2. Materials

The surfactant used in our experiments is sodium dodecyl sulfate (SDS) purchased from Fisher (certi-

fied for electrophoresis and HPLC). The solutions were prepared with deionized water obtained by means of a Millipore unit. They also contained 0.128 M NaCl.

2.3. Preparation of the capillaries

We performed experiments with two types of glass capillaries: a hydrophilic capillary and a hydrophobic capillary with a hydrophilic tip. The latter will be referred to in the text briefly as the hydrophobic capillary. Commercial micropipettes of volume 2 μl and length 3.20 cm (DADE Division American Hospital Supply Co.) have been used as the hydrophilic capillaries. The inner radius of the capillaries were $141 \pm 1.5 \mu\text{m}$. We prepared the hydrophobic capillaries by hydrophobization of the same micropipettes. For this purpose, clean, dry micropipettes were immersed in a 10 wt.% solution of dichlorodimethylsilane (Aldrich) in toluene. After 1 h, the capillaries were rinsed consecutively with absolute toluene, ether, methanol, and finally with distilled water. In order to make the hydrophilic capillary tip, we cut the capillaries. The final capillary length was about 2.5–3 cm. An alternative hydrophobization procedure was also used. The micropipettes, together with several drops of hexamethyldisilazane (Wako), were placed in a small tightly closed vessel for 1 day. The capillaries were then rinsed with distilled water, cut and used for the experiments. Both hydrophobization procedures gave equally good results.

2.4. Calculation of the surface tension

We have calculated the dynamic surface tension by use of the formula

$$\sigma = (P_m - \Delta\rho gh)R_c/2 \quad (1)$$

where P_m is the maximum pressure, $\Delta\rho gh$ is the hydrostatic pressure, $\Delta\rho = \rho_w - \rho_a = 1 \text{ g cm}^{-3}$ is the density difference between water and air, $g = 981 \text{ cm s}^{-2}$ is the gravity, h is the depth of immersion of the capillary tip in the liquid and R_c is the radius of the capillary. The maximum pressure was measured by a calibrated pressure sensor with a precision of 25 dyn cm^{-2} . The depth h was typically $0.7 \pm 0.01 \text{ cm}$, measured directly by a long-

focus microscope. The precision of determination of the DST was about 0.6 dyn cm^{-1} .

2.5. Calculation of the bubble area

We have calculated the area of the bubble surface $A(t)$ by use of the formula for a spherical segment

$$A = \pi(H^2 + R_c^2)$$

where H is the height of the bubble (see Fig. 1(b)). The latter was measured from the video record by an image analyzer (Zeiss Videoplan) with an accuracy of $2 \mu\text{m}$.

3. Results and discussion

In order to adjust the experimental conditions, we have measured the DST of deionized water. Since there is no surfactant in the liquid phase, the surface tension must not depend on the bubbling frequency and must be equal to that measured by static methods. We found that the measured DST at a small chamber volume (approximately 0.5 cm^3) deviated significantly (up to 10%) from the literature value of 71.1 dyn cm^{-1} [11]. We suppressed these deviations by increasing the chamber volume to 10.5 cm^3 . We had to increase also the resistance of the hydrophobic capillary by use of valve 2 to ensure the bubbling of distinct single bubbles. As a result, deviations from the literature value were less than 1% in the frequency range $0\text{--}14 \text{ bubbles s}^{-1}$, which was within the accuracy of a single measurement (see Fig. 2).

3.1. Effect of wettability of the capillary

Pictures of the bubble during its growth are shown in Fig. 3. There is a significant difference between bubble growth in the case of the hydrophobic capillary (Figs. 3(a)–3(c)) and the hydrophilic capillary (Figs. 3(d)–3(f)). The base of the bubble is fixed to the tip of the hydrophobic capillary from the beginning of its growth until its detachment, whereas the “bubble” is inside the hydrophilic capillary at the beginning (Fig. 3(d)). This confirms the observations of other workers [3,4,9]. The wettability of the capillary has a

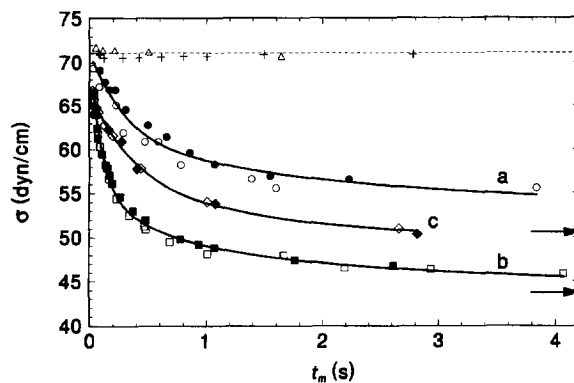


Fig. 2. Dynamic surface tension of pure water (+, Δ) and SDS solutions at concentrations equal to (curve a) $2 \times 10^{-4} \text{ M}$ and (curves b, c) $4 \times 10^{-4} \text{ M}$ in the presence of 0.128 M NaCl measured with a hydrophilic capillary (+; curves a, b) and with a hydrophobic capillary (Δ ; curve c). The filled and empty symbols correspond to different runs. The arrows indicate the respective equilibrium values of the surface tension taken from Ref. [16]. The broken line corresponds to the surface tension of pure water. The solid lines are the best fits with the real law of surface expansion (see appendix).

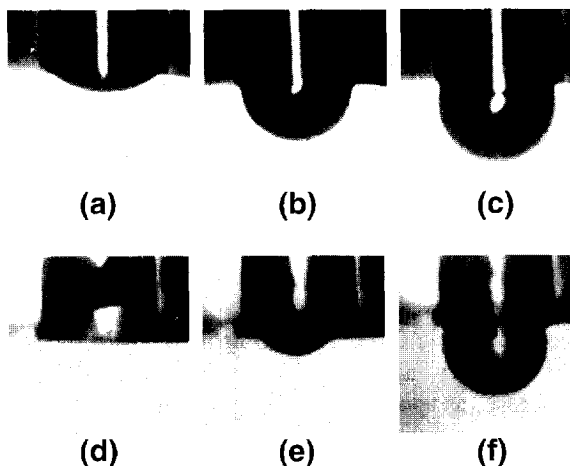


Fig. 3. Consecutive photographs of a growing bubble in the case of (a)–(c) a hydrophobic capillary and (d)–(f) a hydrophilic capillary immersed in $4 \times 10^{-4} \text{ M SDS}$ solution.

pronounced effect on the expansion of the bubble area shown in Fig. 4. There, the bubble area $A(t)$ is scaled by the cross-sectional area of the capillary A_c , whereas the time t is scaled by the total lifetime of the bubble τ . Hence, $A/A_c = 1$ corresponds to a flat surface while $A/A_c = 2$ corresponds to a hemispherical bubble. The initial area of the bubble

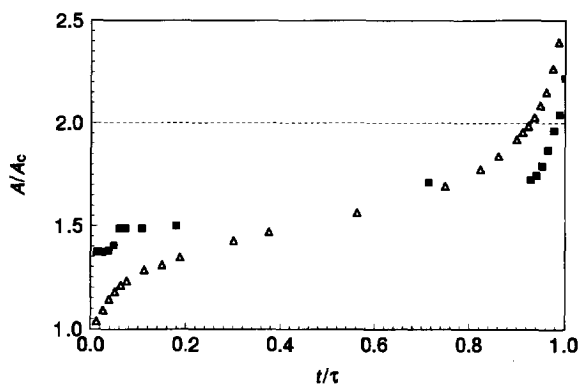


Fig. 4. Comparison of the dimensionless areas of single bubbles obtained with (Δ) a hydrophobic capillary and (\blacksquare) a hydrophilic capillary in 4×10^{-4} M SDS solution for bubbling periods of 2.86 s and 2.67 s, respectively.

obtained with the hydrophilic capillary is about 1.5 times greater than that measured with the hydrophobic capillary. In contrast to the case of the hydrophobic capillary, the area of the bubble at the hydrophilic capillary does not change appreciably during almost 90% of the total life-time of the bubble. The DSTs of the 4×10^{-4} M SDS solution measured with capillaries of both types are plotted in Fig. 2. Although both capillaries give correct values for the DST of pure water, there is a distinct difference between the DSTs of the surfactant solution. The DST measured with the hydrophilic capillary (diamonds) is about 5 dyn cm^{-1} higher than the values obtained with the hydrophobic capillary (squares) except at very short times.

3.2. Effect of surfactant on the bubble expansion

The dimensionless area of the bubbles obtained with the hydrophobic capillary is plotted versus the dimensionless time in Fig. 5. The coincidence of the curves obtained at different bubbling periods implies a general validity of the area expansion law for a given concentration. The curves obtained in the presence of surfactant have a greater slope than that obtained without surfactant, except for the period of fast post-hemispherical expansion of the bubble ($A/A_c > 2$). The larger slopes are probably due to a lowering of the surface tension caused by the adsorption of surfactant, thus facilitating

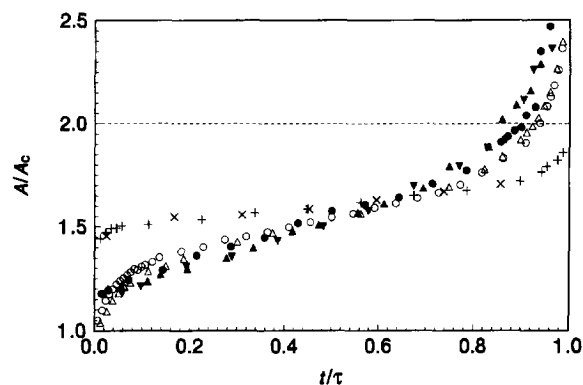


Fig. 5. The dimensionless area of single bubbles versus the dimensionless time for (+, \times) pure water and SDS solutions at concentrations equal to 2×10^{-4} M (filled symbols) and 4×10^{-4} M (empty symbols) in the case of the hydrophobic capillary for bubbling periods τ (s) of (+) 2.97, (\times) 1.40, (\bullet) 2.33, (\blacktriangledown) 1.73, (\blacktriangle) 1.2, (\circ) 4.17 and (Δ) 2.67.

bubble growth. As a result, the bubbles reach a hemispherical shape ($A/A_c = 2$) earlier with surfactant present than in pure water. In order to verify if the maximum pressure corresponds exactly to a hemispherical shape of the bubble, we have compared the pressure profiles documented by oscillograms with the video record of the growth of single bubbles. A typical oscillogram obtained at a long bubbling period ($\tau = 4.17$ s) is shown in Fig. 6. There, the transient pressure P is scaled by its maximum value P_m . The pressure increases linearly until it reaches its maximum at a time t_m , after which P decreases very fast to its minimum value, which corresponds to the detachment of the bubble. In the same figure the height H is plotted of the same bubble measured from the video record. The bubble becomes a hemisphere ($H/R_c = 1$) with a radius $R = R_c$ at time t_h . It is seen that the bubble is not a hemisphere at the moment of maximum pressure t_m ($H/R_c > 1$) but has a radius R_m greater than the capillary radius. The respective analysis for other bubbling periods studied has been simplified in the following manner. We have measured the duration of the post-hemispherical bubble growth t_d , i.e. the time that had elapsed from the moment t_h until the detachment of the bubble. Usually t_d is called the “dead” time [1,11–13]. We have also measured the duration of the pressure drop t_{dp} (see Fig. 6). It is obvious that

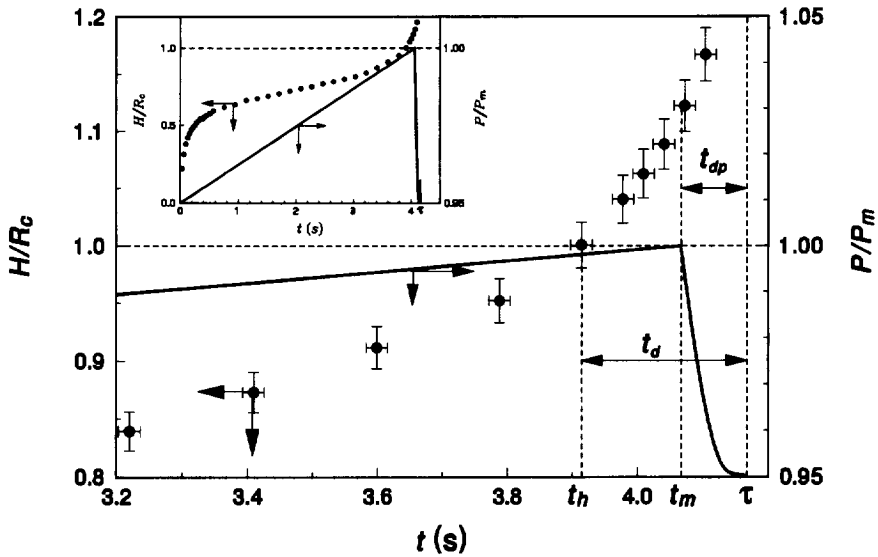


Fig. 6. Dimensionless height of the bubble H/R_c (circles) and dimensionless pressure P/P_m (solid line) versus the expansion time t obtained in 4×10^{-4} M SDS solution.

the maximum pressure will correspond to a hemispherical bubble only if $t_d = t_{dp}$. However, the radius of the bubble will be greater than the capillary radius at the moment of maximum pressure if $t_d > t_{dp}$. The values of t_d (measured from video records) and t_{dp} (measured from oscillograms) are compared in Fig. 7. It is seen that for pure water, t_d (filled squares) and t_{dp} (empty squares) coincide in the range of experimental error

for all bubbling periods. Hence, the maximum pressure corresponds exactly to a hemispherical bubble. This is not the case in the presence of surfactant. The post-hemispherical bubble growth period t_d is significantly greater than t_{dp} at bubbling periods larger than 0.7 s. Hence, the bubble is greater than a hemisphere at the moment of maximum pressure. The deviation of the bubble radius R_m from the capillary radius R_c increases at large bubbling periods. This is in agreement with the theoretical prediction of Garret and Ward [4]. The observed phenomena can be explained in the following way. In the case of pure liquids, the capillary pressure P_c changes during the expansion only due to the change of the bubble radius R (σ is a constant). Hence, P_c and R must reach their extreme values simultaneously. In the presence of surfactants, however, P_c depends also on σ which changes all the time due to the surfactant adsorption. In general, there is no reason for any coincidence between extremums of R and σ . That is why the maximum capillary pressure may not correspond to the minimum bubble radius, i.e. to R_c . A similar conclusion has been drawn in Ref. [4], but has not been proved by experiments with any degree of certainty. Our results throw new light on the validity of Eq. (1), which is widely used in the

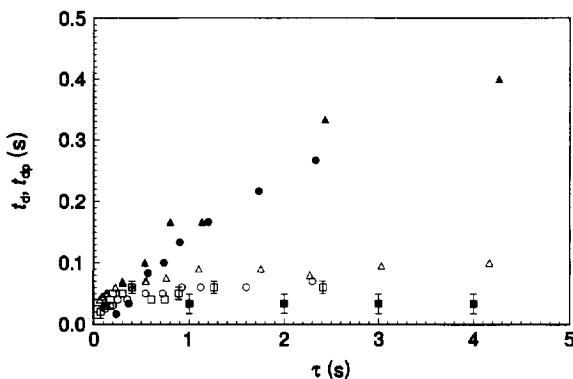


Fig. 7. The duration of the post-hemispherical bubble expansion t_d (filled symbols) and the duration of the pressure drop t_{dp} (empty symbols) versus the bubbling period τ for squares pure water, (circles) 2×10^{-4} M SDS and (triangles) 4×10^{-4} M SDS.

literature [1,3,10–15]. It turns out that Eq. (1) is strictly valid for pure liquids, and probably for surfactant solutions at short bubbling periods (less than 0.5 s in our case). However, R_c in Eq. (1) should be replaced by R_m ($R_m > R_c$) at long bubbling periods. We have found that R_m measured from video records at long bubbling periods does not exceed the capillary radius R_c by very much. The bubble radius R_m differs from R_c by less than 2% at the lower SDS concentration and by less than 1% with the more concentrated SDS solution. That is why we used R_c instead of R_m for the calculation of $\sigma(t)$. This lead to an error in the DST of less than 1 dyn cm^{-1} , which was acceptable in our case. This effect seems to be more important at low surfactant concentrations and bubbling periods longer than 4–5 s, but additional studies are needed for the elucidation of this problem.

3.3. Effect of the surface expansion on the interpretation of the DST data

The dynamic surface tension of the surfactant solutions is plotted as a function of the time t_m in Fig. 2. We have measured t_m directly from the oscillograms. The data points tend to the surface tension of pure water at zero time, while they tend to the respective equilibrium values of the surface tension at infinite time. As expected, the DST obtained at the lower surfactant concentration is always higher than the DST obtained at the higher concentration. We have interpreted these data by use of the theory of Kralchevsky et al. [12] (for a brief outline of the theory, see the appendix). Their theory concerns large deviations from equilibrium and requires the total deformation of the surface $\alpha = \ln[A(t)/A(0)]$ to be known. We have found that the following function

$$\alpha = b_1 \left[\tan b_2 + b_3 \frac{t}{\tau} + \tan \left(b_4 \frac{t}{\tau} - b_2 \right) \right] \quad (2)$$

fits well the deformation curves recalculated from the experimental data shown in Figs. 4 and 5. The coefficients b_i depend on the surfactant concentration. They are $b_1 = 0.0686$, $b_2 = 0.8685$, $b_3 = 4.7431$ and $b_4 = 2.3325$ for the 2×10^{-4} M SDS solution; and $b_1 = 0.0511$, $b_2 = 1.4245$, $b_3 = 3.6223$

and $b_4 = 2.8896$ for the 4×10^{-4} M SDS solution. The theory [12] also requires the adsorption isotherm of the surfactant. We used the isotherm of SDS obtained by Tajima [16], as did the authors of Ref. [12], but we leave the limiting area per molecule A_∞ (the reverse of the saturation adsorption, Γ_∞) as an adjustable parameter in our computations. The other adjustable parameters in the numerical fits are the same as in Ref. [12]: the initial adsorption $\Gamma_0 = \Gamma(0)$ and the diffusivity of the surfactant molecules D . The theoretical model describes the experimental data well, as seen in Fig. 2. In order to verify the importance of the surface expansion, we have processed the DST data obtained with the hydrophobic capillary assuming the different laws of bubble expansion shown in Fig. 8. Beside the real time dependence of the bubble area (curve 1) we have fitted the experimental DST dependences assuming also a constant volume rate of bubble growth (curve 2), a linear increase of the bubble surface (curve 3) and a constant bubble area (curve 4). The values of Γ_0 , A_∞ , D and the standard deviations of the best fits are summarized in Table 1. The fits at the higher SDS concentration (4×10^{-4} M) are more reliable because their standard deviations are smaller than those at the lower concentration. In the former case, the worst fit is obtained assuming

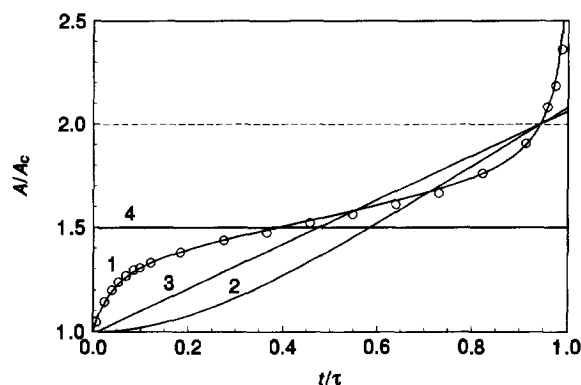


Fig. 8. Models for the expansion of the bubble area A used for interpretation of the DST data: the best fit of the experimentally measured area according to Eq. (2) (curve 1), an expansion under a constant flow rate (curve 2), a linear surface expansion (curve 3) and a constant bubble area (curve 4). The circles represent data measured with a hydrophobic capillary at 4×10^{-4} M SDS.

Table 1

Properties of SDS solutions computed with the laws of bubble surface expansion shown in Fig. 8 in the case of a hydrophobic capillary^a

Law of expansion ^c	$10^6 D$ ($\text{cm}^2 \text{s}^{-1}$)	$10^{10} \Gamma_0$ (mol cm^{-2})	$10^{15} A_\infty$ (cm^2)	Standard deviation (dyn cm^{-1})	D/D_e
$c = 2 \times 10^{-4} \text{ mol l}^{-1}$					
1	7.0	1.4	3.0	1.0	1.27
2	9.1	1.3	2.8	1.0	1.66
3	8.2	1.9	2.8	1.0	1.49
4	3.5	1.0	2.6	0.9	0.64
$c = 4 \times 10^{-4} \text{ mol l}^{-1}$					
1	5.6 (0.6) ^b	2.2 (2.8) ^b	2.6 (2.7) ^b	0.4 (0.4) ^b	1.02 (0.11) ^b
2	8.6	2.0	2.5	0.4	1.56
3	7.7	2.8	2.5	0.4	1.40
4	2.3	1.6	2.4	0.7	0.42

^a Expected value $D_e = 5.5 \times 10^{-6} \text{ cm}^2 \text{ s}^{-1}$ [17].^b Values obtained with a hydrophilic capillary.^c See text and Fig. 8.

a constant bubble area (i.e. without expansion). The values of A_∞ are very close to or coincide with the value $2.5 \times 10^{-15} \text{ cm}^2$ obtained in Ref. [16]. The initial adsorptions Γ_0 are not equal to zero. This is in accordance with the findings of another worker [1]. The lower Γ_0 corresponds to the more dilute surfactant solution in each particular case of surface expansion, which seems reasonable. The calculated diffusivities D are compared with the expected value $D_e = 5.5 \times 10^{-6} \text{ cm}^2 \text{ s}^{-1}$ [17], in the last column of Table 1. The diffusivity obtained with the real law of bubble expansion (1) is closest to the expected value, whereas D calculated with a constant flow rate (2) or with a linear surface expansion (3) is about 1.5 times greater than D_e . The worst result is obtained when the surface expansion has been neglected (4). Hence, the expansion of the bubble surface should be taken into account for the proper interpretation of the DST data. One can conclude that the law of bubble expansion has a significant effect on the interpretation of the DST data obtained with the hydrophobic capillary.

We have also processed the data obtained with the hydrophilic capillary using the real law of surface expansion shown in Fig. 4. The results are also given in Table 1 (the values in parentheses). Although the values of Γ_0 and A_∞ are close to those obtained with the hydrophobic capillary, the value of D is about 10 times lower. This is in

accordance with the results obtained by Bendure [3] for some non-ionic surfactants. Our results suggest that the surface expansion is not of primary importance for interpretation of the DST data obtained with the hydrophilic capillary. The most important factor seems to be the motion of the "bubble" (the meniscus) inside the hydrophilic capillary observed at the beginning of the bubble growth process (Fig. 3(d)).

4. Conclusions

The wettability of the capillary has a strong effect on the DST of the surfactant solutions measured by the MBPM. The DST measured with the hydrophilic capillary is significantly higher than the respective values for the hydrophobic capillary. This can be attributed to the more restricted conditions for surfactant adsorption due to the motion of the "bubble" inside the hydrophilic capillary.

The expansion of the bubble surface is affected by the surfactant. The bubble radius is greater than the capillary radius at the moment of maximum pressure in the surfactant solutions. This effect is more pronounced in dilute solutions for long bubbling periods. However, it can be neglected at bubbling periods shorter than several

seconds, which does not lead to a significant error in the DST.

The real law of bubble expansion is non-trivial and differs substantially from the expansion under a constant flow rate or from the linear surface expansion as commonly assumed in the literature. The best interpretation of the DST data is achieved when the real law of expansion is used in the case of a hydrophobic capillary. The other two models for the bubble expansion give worse results, but are better than the model without expansion. Hence, the real law of bubble expansion should be used for the proper interpretation of the DST data obtained with the hydrophobic capillary. In contrast, the surface expansion is not of primary importance for the interpretation of the DST data obtained with the hydrophilic capillary. The value of D calculated with the real law of bubble expansion is one order of magnitude lower than the expected value. The most important factor seems to be the motion of the “bubble” (the meniscus) inside the hydrophilic capillary observed at the beginning of the bubble growth process.

Acknowledgements

We acknowledge the assistance of Mrs. E. Basheva and Mrs. S. Kralchevska in performing part of the measurements. We are indebted to Professor I.B. Ivanov for helpful discussions. The Colgate–Palmolive Co. is gratefully acknowledged for financial support of this work.

References

- [1] K.J. Mysels, *Colloids Surfaces*, 43 (1990) 241.
- [2] V.B. Fainerman, A.V. Makievski and R. Miller, *Colloids Surfaces A: Physicochem. Eng. Aspects*, 75 (1993) 229.
- [3] R.L. Bendure, *J. Colloid Interface Sci.*, 35 (1971) 238.
- [4] P.R. Garret and D.R. Ward, *J. Colloid Interface Sci.*, 132 (1989) 475.
- [5] R.S. Hansen, *J. Phys. Chem.*, 64 (1960) 637.
- [6] P. Joos and E. Rillaerts, *J. Colloid Interface Sci.*, 79 (1981) 96.
- [7] J. Kloubek, *J. Colloid Interface Sci.*, 41 (1972) 1.
- [8] V.B. Fainerman, A.V. Makievski and P. Joos, *Zh. Fiz. Khim.*, 67 (1993) 452.
- [9] K.J. Mysels, *Langmuir*, 2 (1986) 428.
- [10] X.Y. Hua and M.G. Rosen, *J. Colloid Interface Sci.*, 124 (1988) 652.
- [11] R.C. Weast (Ed.), *Handbook of Chemistry and Physics*, 55th edn., CRC Press, Boca Raton, FL, 1974, p. F-43.
- [12] P.A. Kralchevsky, Y.S. Radkov and N.D. Denkov, *J. Colloid Interface Sci.*, 161 (1993) 361.
- [13] M. Austin, B.B. Bright and E.A. Simpson, *J. Colloid Interface Sci.*, 23 (1967) 108.
- [14] F. Wolf and F. Sauerwald, *Kolloid.-Z.*, 118 (1950) 1.
- [15] R. Miller, P. Joos and V.B. Fainerman, *Adv. Colloid Interface Sci.*, 49 (1994) 249.
- [16] K. Tajima, *Bull. Chem. Soc. Jpn.* 43 (1970) 3063.
- [17] N. Kamenka, B. Lindman and B. Brun, *Colloid Polym. Sci.*, 252 (1974) 144.

Appendix

According to the theoretical model developed in Ref. [12], the surface tension can be calculated by solving the following set of equations

$$\sigma(t) = \sigma_0 + 6.03\sqrt{c_i} + k_B T \times \left[0.43\Gamma - \left(\frac{1}{\Gamma} - \frac{1}{\Gamma_\infty} \right)^{-1} \right] \quad (\text{A1})$$

$$c(t) = 2.1795 \times 10^{-8} \left(\frac{\Gamma_\infty}{\Gamma} \right)^{0.43} \left(\frac{\Gamma_\infty}{\Gamma} - 1 \right)^{-1} \times \exp\left(\frac{\Gamma}{\Gamma_\infty - \Gamma} \right) \quad (\text{A2})$$

$$\Gamma(t) = c_e l + (\Gamma_0 - c_e l_0) \exp(-\alpha) \quad (\text{A3})$$

$$l \frac{dl}{dt} + l^2 \dot{\alpha} = \left(\frac{\pi}{2} - 1 \right) D \left(1 - \frac{c}{c_e} \right)^2 \quad (\text{A4})$$

$$\alpha = b_1 \left[\tan b_2 + b_3 \frac{t}{\tau} + \tan \left(b_4 \frac{t}{\tau} - b_2 \right) \right] \quad (\text{A5})$$

at $0 \leq t \leq t_m$

where σ_0 is the surface tension of pure water; c_i is the electrolyte concentration expressed in moles per litre, k_B is the Boltzman constant, $\Gamma(t)$ is the surfactant adsorption, $\Gamma_\infty = 1/A_\infty$ is the saturation adsorption, $\Gamma_0 = \Gamma(0)$ is the initial adsorption, $c(t)$ is the subsurface concentration (the concentration of surfactant close to the bubble surface), c_e is the equilibrium surfactant concentration, D is the diffusivity of the surfactant molecules, $\dot{\alpha} = d(\ln A)/dt$ is the rate of bubble expansion, $l(t)$ is

the thickness of the subsurface layer (i.e. the layer adjacent to the bubble surface, where the surfactant concentration differs appreciably from the equilibrium concentration, $l_0 = l(0)$ is the initial thickness of the subsurface layer, and t_m is the life-time of the bubble surface corrected for deadtime. Eq. (A1) is an empirical equation of state proposed by Tajima [16] for SDS in the presence of univalent electrolyte.

To solve Eqs. (A1)–(A5), we first computed $\alpha(t)$ by processing the experimental data for the bubble

area. After that, we solved the set of equations for the unknown functions $l(t)$, $\Gamma(t)$, $c(t)$ and $\sigma(t)$ by numerical integration under the initial condition $l(0)=0$. Since the initial adsorption is not exactly known, we used Γ_0 as an adjustable parameter together with the saturation adsorption Γ_∞ and the diffusivity D . For given $(\Gamma_0, \Gamma_\infty, D)$ the numerical problem is solved for each value of t_m , and the calculated values for σ are then compared with the set of experimental values by the least-squares method.